

A smart nanofibrous material for adsorbing and detecting elemental mercury in air

Antonella Macagnano¹, Viviana Perri^{1,2}, Emiliano Zampetti¹, Andrea Bearzotti¹, Fabrizio De Cesare^{1,3},
Francesca Sprovieri⁴, Nicola Pirrone¹

5 ¹Institute of Atmospheric Pollution Research-CNR, Via Salaria km 29,300 Montelibretti 00016 (RM), Italy;

²University of Calabria, via Pietro Bucci, Arcavacata, Rende 87036 (CS), Italy;

³DIBAF-University of Tuscia, Via S. Camillo de Lellis, 01100 Viterbo, Italy;

⁴Institute of Atmospheric Pollution Research-CNR, Division of Rende, c/o UNICAL-Polifunzionale Arcavacata, Rende
87036 (CS) Italy;

10

Correspondence to: Antonella Macagnano (a.macagnano@iia.cnr.it; antonella.macagnano@cnr.it)

Abstract. The combination of gold affinity for mercury with nanosized frameworks has allowed to design and fabricate novel kinds of sensors with promising sensing features for environmental applications. Specifically, conductive sensors based on composite nanofibrous electrospun layers of titania easily decorated with gold nanoparticles were developed to
15 obtain nanostructured hybrid materials, capable of entrapping and revealing GEM traces from environment. The electrical properties of the resulting chemosensors were measured. Few minutes of air sampling were sufficient to detect the concentration of mercury in the air, in the range between 20-100 ppb, without using traps or gas carriers (LOD \square 1.5 ppb). Longer measurements allowed the sensor to detect lower concentrations of GEM. The resulting chemosensors are expected to be low-cost, very stable (due to the peculiar structure), and requiring low power, low maintenance and simple equipment
20 to work.

1 Introduction

Mercury (Hg) is released into the atmosphere both by human's activities, predominantly fossil fuel combustion, and naturally, for example, from soil out-gassing, volcanoes and evasion from the sea (Pirrone et al., 2010; Pacyna et al., 2010). One of the more troublesome questions in recent years has been to quantify not only the strength of emission sources but
25 also the effects of re-emission of previously deposited Hg on the overall distribution, concentration and speciation of Hg in the atmosphere (Hedgecock et al., 2003). The deposition of atmospheric Hg depends on its chemical speciation, where the term speciation is used to distinguish between the gaseous elemental (GEM) and gaseous oxidized forms of Hg (GOM and Particle bound mercury-PBM) and their chemical-physical characteristics (Lyman et al., 2010; Sprovieri et al., 2016a,b). To be precise, total gaseous mercury (TGM) mainly comprises GEM with minor fractions of other volatile species (e.g., HgO,
30 HgCl₂, HgBr₂, CH₃HgCl, or (CH₃)₂Hg). However, in spite of conceptual differences between TGM and GEM, they have often been used without clear distinction. This was allowable to a degree as the predominant fraction of TGM (usually in

excess of 99%) is often represented by GEM under normal conditions. GEM is relatively inert under atmospheric conditions, only slightly soluble and also quite volatile, whereas several oxidized Hg forms found in the atmosphere are both soluble and involatile, thus they are efficiently scavenged and consequently deposited by liquid atmospheric water, such as rain and fog droplets, but also deliquesced aerosol particles. The dispersion of GEM on global scale therefore, depends on the rate of its oxidation in the atmosphere as this determines its long atmospheric lifetime (generally >1 year), limiting local emission controls from protecting all environments. Several international initiatives and programs (i.e., the United Nations Environment Program (UNEP)) have also made a tremendous effort in identifying and quantifying Hg pollution across the globe, especially the “hot-spots”, aimed at reducing risk of exposure to this neurotoxin pollutant. Policy makers are working toward a worldwide effort for supporting the constructing an accurate global Hg budget and to model the benefits or consequences of changes in Hg emissions, for example, as proscribed by the Minamata Convention. Anticipating a global policy, in 2010 the European Commission began a five-year project called the Global Mercury Observation System (GMOS, www.gmos.eu) to create a coordinated global network to gaps in emissions monitoring and in the spatial coverage of environmental observations, mostly in the tropical regions and Southern Hemisphere, thus adequate for improving models and making policy recommendations (Sprovieri et al., 2016a,b). To date the GMOS network consists of more 43 monitoring stations worldwide distributed including high altitude and sea level monitoring sites, and located in climatically diverse regions, including polar areas (Sprovieri et al., 2016a,b). One of the major outcomes of GMOS has been an interoperable e-infrastructure developed following the Group on Earth Observations (GEO) data sharing and interoperability principles which allows us to provide support to UNEP for the implementation of the Minamata Convention (i.e., Article 22). GMOS activities are currently part of the GEO strategic plan (2016–2025) within the flagship on “tracking persistent pollutants”. The overall goal of this flagship is to support the development of GEOSS (Global Earth Observation System of Systems) by fostering research and technological development on new advanced sensors for in situ and satellite platforms, in order to lower the management costs of long-term monitoring programs and improve spatial coverage of observations. Since automated measurement methods of Hg often require power, carrier gases like argon, and significant operator training, they are difficult to apply for understanding Hg air concentrations and deposition across broad regional and global scales. Therefore, the lack of an inexpensive, stand-alone, low power, low-maintenance sensor is a primary technical issue to be solved for the sustainability of a global network such as GMOS. Previous research highlighted that Hg-concentration levels in air vary greatly across different environmental locations, remote as the Polar Regions, background or rural, and urban locations with an average range between 1.5 ngm^{-3} (GEM) and 1 pgm^{-3} (gaseous oxidized Mercury-GOM and particle bound mercury-PBM), depending on the speciation. Hence, for the determination of atmospheric Hg also at such low levels, sampling and analytical methods should be sensitive enough to quantify the concentration profiles of diverse Hg species in each respective environmental setting to better understand their environmental behavior and patterns. Fortunately, many advances made in analytical methodologies have made it possible to study atmospheric Hg in different environmental locations. However, several limitations and difficulties have still experienced in Hg analysis, as most methods cannot yet directly or accurately determine minor Hg species (Gustin et al., 2013). Hence, efforts should be continued to secure further

the reliability, the traceability, and the accuracy of Hg levels measured in air. Current air monitoring devices are amply sensitive to detect the global background but are costly, complicated configuration, electricity requirements and high maintenance. A further limitation is the ultra-low levels of ambient mercury in the atmosphere. The typical background gaseous elemental mercury (GEM) level of 1.5 ng/m³ is equivalent to 168 parts per quadrillion by volume (ppq_v). There is no other atmospheric compound being measured routinely, continuously and automatically at this ultra-low concentration. These features limit the scientific research community's ability to long-term measure atmospheric Hg concentrations worldwide. Sampling and analysis of atmospheric Hg is made most commonly as GEM/TGM because of their greater abundance, even if both manual and automatic methods have been currently developed for different Hg forms to suit the measurement and monitoring application. The most common sampling method employed relies on adsorption on gold amalgam and then, either directly or indirectly, through a stepwise process of thermal desorption and final detection [usually by cold-fiber atomic absorption spectroscopy (CVAAS) or cold-fiber atomic fluorescence spectroscopy (CVAFS)]. However, our knowledge presents currently several gaps to be solved. Firstly, the atmospheric chemistry of Hg remains poorly understood, especially the oxidation pathways by which GEM is converted to GOM, the reduction pathway which converts GOM back to GEM, and the gas-particle partitioning. This is partially due to the need for identification of the chemical forms of oxidized Hg in the atmosphere and methods to measure these compounds individually. In addition, the limitations and potential interferences with our current measurement methods have not been adequately investigated, thus alternate methods to measure atmospheric Hg are needed. Given the uncertainty and restrictions associated with automated and/or semi-automated Hg measurements (Gustin et al., 2013; Pirrone et al., 2013), and above all, responding to the technical needs of an expanding Hg global observation network, we developed a reliable, sensitive, and inexpensive surface for atmospheric Hg detection. In particular, we investigated and demonstrated the utility of composite nanofibrous electrospun layers of titania decorated with gold nanoparticles (AuNPs) to obtain nanostructured materials capable of adsorbing GEM as a useful alternative system for making regional and global estimates of air Hg concentrations. Methods and new sampling systems previously developed, such as passive samplers, have been used to understand long-term global distribution of persistent organic pollutants (POPs) (Harner et al., 2003; Pozo et al., 2004). Other passive samplers for both TGM and GOM collection on the basis of diffusion have been constructed using a variety of synthetic materials (i.e., gold and silver surfaces, and sulfate-impregnated carbon) and housings (Lyman et al., 2010; Gustin et al., 2011; Zhang et al., 2012; Huang et al., 2014). However, because of the differences in design of passive samplers, ambient air Hg concentrations quantified by various samplers may not be comparable. In addition, sampling rates (SRs) using the same passive samplers may depend on environmental conditions and atmospheric chemistry at each site. Moreover, it has been also highlighted that the performance of passive samplers may be influenced by meteorological factors (e.g., T °C, RH, wind speed) therefore inducing bias for the result of passive sampling (Plaisance et al., 2004; Sderstrm et al., 2004). On the other hand, incentive for developing simple and cost-effective samplers that are capable of monitoring over an extended period and require no technical expertise for deployment of these systems also at remote locations is now obvious. In this work we describe an alternative approach adopted in the place of conventional ones demonstrating that the combination of gold affinity for Hg

with a nanoscale sized framework of titania provided the chance to create promising sensors for environmental monitoring in real time, characterised by high sensitivity to the analyte. The novel sensor is a relatively simple and low cost method for measurement of the most abundant Hg form in ambient air (TGM/GEM) due to reusable parts and simple deployment steps. Further, we have evaluated the applicability of this measurement technique with respect to real environmental conditions highlighting future directions of research on airborne Hg determination. The TGM/GEM sensor surface described here could be deployed in a global network such as GMOS; a permanent network of ground based monitoring sites and observations of Hg and/or related species on a global scale and with remote sensors would in fact be highly desirable. These data are needed to test and validate model processes and predictions, understand the source-receptor relationships, understand long-term changes in the global Hg cycle, and at least, would help policy makers to set regulations for different areas. The sensor features are related to the nanofibrous scaffold of titania capable of growing up gold nano-aggregates by photocatalysis, tunable in size and shape. Such a nanostructured layer, fabricated by electrospinning technology, firstly improves sensor features with respect to those of compact films, by enhancing the global number of binding sites of analyte-sensor and reducing some bulk drawbacks. Secondly, the combination of metal oxides and metal nanostructures, improves the sensitivity, allows sensor to work at room temperature, tunes selectivity towards different gas species by adjusting the surface to volume ratio of nanosized structures and affect sensor lifetime. Morphological, optical, electrical aspects and sensing measurements of fibers of GEM in air have been reported and discussed. When designed, the resulting Hg adsorbent material was expected to be suitable for novel Hg sensors fabrication, since a similar nanofibrous scaffold doped with AuNPs was described in literature as filtering systems capable of adsorbing and removal Hg vapor from the environment with an efficiency of about 100% (Y Yuan et al., 2012). In fact, in previous works (Macagnano et al., 2017 and 2015a) the authors reported a high sensitivity of the sensor, capable to detect up to dozens ppt., despite of a long time necessary to reveal the analyte at these concentrations, in air. In this work the chance to apply the sensor in polluted sites and in real time has been presented and described.

2 Materials and methods

2.1 Chemicals

All chemicals were purchased from Sigma-Aldrich and used without further purification: polyvinylpyrrolidone (PVP, Mn 1,300,000), titanium isopropoxide (TiiP, 99.999%), gold (III) chloride hydrate (HAuCl_4 , 99.999%), anhydrous ethanol (EtOH_a) and glacial acetic acid (AcAc_g). Ultrapure water ($5.5 \cdot 10^{-8} \text{ Scm}^{-1}$) was produced by MilliQ-EMD Millipore.

2.2 Electrospinning technology

Electrospinning (ES) is a widely used technique for the electrostatic production of nanofibers, during which an electric field is used to make polymer fibers with diameters ranging from 2 nm to some micrometres from polymer solutions (or melts). It is currently the most economic, versatile, and efficient technology to fabricate highly porous membranes made of nano-

and/or microfibers also for sensors (Macagnano et al., 2015b). It is based on the application of a high voltage difference between a spinneret ejecting a polymeric solution and a grounded collector. The jet of solution is accelerated and stretched by the external electric field while travelling towards the collector, leading to the creation of continuous solid fibers as the solvent evaporates. The electrospinning apparatus used in the present study (designed and assembled in CNR laboratories) comprised a home-made clean box equipped with temperature and humidity sensors, a syringe pump (KDS 200, KD Scientific) and a grounded rotating cylindrical collector (45 mm diameter), a high voltage oscillator (100 V) driving a high voltage (ranging from 1 to 50 kV) and a high power AC-DC (alternative current-direct current) converter. Electrospinning solution ($7.877 \cdot 10^{-5}$ M) was prepared by dissolving PVP in EtOH_a and stirring (2 hours). A 2 ml aliquot of 1:4 (w/v) solution of TiiP solved in 1:1 (v/v) mixture of AcAc_g and EtOH_a was freshly prepared and added to 2.5 ml PVP solution under stirring in order to obtain a 1.95 (w/w) TiiP/PVP final ratio. Both mixtures were prepared in a glove box under low humidity rate (<7% RH). The syringe filled with the TiiP/PVP solution and housed in the syringe pump, was connected to a positive DC-voltage (6 kV), and set perpendicular to a 15 cm far grounded rotating collector. The substrates were fixed through suitable holders onto the collector (600 rpm, 21 °C and 35% RH) and processed (feed rate 150 ml h⁻¹) for 20 min to obtain scaffolds for sensors. After deposition, PVP/TiO₂ composite nanofibers were left for some hours at room temperature to undergo fully self-hydrolysis of TiiP (Li et al., 2003) and then annealed under oxygen atmosphere (muffle furnace) using a thermal ramp from room temperature up to 550 °C (1 °C min⁻¹, 4 h dwell time) in order to remove PVP and crystallize the metal oxide (*anatase*).

2.3 Transducers: interdigitated electrodes

The transducer adopted in the present work to convert the physico-chemical interactions of analytes with the different polymer fibers in an electrical signal was an interdigitated electrode (IDE) (Bakir et al, 1973; James et al., 2013). Specifically, the transducer, which consisted of 40 pairs of electrodes (150 nm in electrode thickness, 20 μm in gap and electrode width and 5620 μm in length), was manufactured in CNR laboratories through a standard photolithographic process (lift-off procedure), then followed by Ti sputtering and Pt evaporation, suitable to generate the electrodes of the size reported above, on a 4 in. oxidised silicon wafer. After electrospinning deposition all the electrical signals of the resulting chemoresistors were recorded by an electrometer (Keithley 6517 Electrometer).

2.4 Titania nanofibers

Upon calcination, the diameters of fibers extraordinarily shrunk: mean diameters of fibers were estimated through image analyses to be approximately within the range of 60–80 nm. Specifically, the resulting fibers appeared fine and rough at surface, with a fairly homogeneous fabric. The absence of beads and the good quality of the long and continuous fibers was confirmed through SEM micrographs. A highly porous and dense network of nanofibers covering the electrodes was observed, showing interconnected void volumes (porosity) and high surface-to-volume ratios (specific surface area).

Zampetti et al., (2013) reported that such a fibrous layer showed a 99% of pores having an area less than $10 \mu\text{m}^2$, with more than 80% pores being $<1 \text{mm}^2$.

2.5 AuNPs/TiO₂NFs photocatalytic decoration

Exploiting the photocatalytic properties of TiO₂, gold nanoparticles were selectively grown, under UV-light irradiation, on the electrospun titania nanofibers through the photoreduction of HAuCl₄ in the presence of an organic capping reagent (PVP). Thus the resulting fibrous scaffolds were dipped into an aqueous solution containing HAuCl₄ and PVP ($1.5 \cdot 10^{-3}\text{M}$ and 0.1M respectively) and exposed to UV light irradiation for specified intervals (UV lamp 365 nm) (Helios, Italquartz). Depending on the gold nanoparticles sizes that were forming in photocatalysis, the dip-solution changed from light yellow to purple. Samples were rinsed extensively with water and then air-dried. Before morphological, electrical and sensing measurements, samples were heated at $450 \text{ }^\circ\text{C}$ per 1 h to eliminate the PVP traces. Morphological characterization were provided by scanning electron microscopy (SEM) (Jeol, JSM 5200, 20 keV) with pictures captured at 5 kV accelerating voltage. AFM (atomic force microscopy) micrographs were taken in tapping mode using 190Al-G tips, 190 kHz, 48N/m (Nanosurf FlexAFM). TEM (C-TEM, control transmission electron microscopy) micrographs were performed at 200 keV with an analytical double tilt probe. TEM specimen were prepared by gently scraping at first the TiO₂ nanofibrous layer electrospun onto the silicon support and then collecting the nanofibers, through adhesion upon contact with holy carbon thin film. UV-Vis spectra were provided by Spectrophotometer UV-2600 (Shimadzu), analyzing quartz slices coated with nanofibers. These substrates were able to collect fibers by electrospinning (20 min), and then were subjected to calcination according to the described above procedure, and then UV irradiation in the aqueous solution. The fibrous layer stayed stuck to the substrate if the thickness was thin enough. Longer depositions caused curling of fibers during the calcination process.

20 2.6 Measurement set-up

The sensor was placed in a suitable PTFE-made measurement chamber (0.7 ml volume) connected to an electrometer (Keithley 6517 Electrometer) capable of both measuring the current flowing through the IDE, when a fixed potential was applied to it, and sending data to a PC. Dynamic measurements were carried out at room temperature both using: (i) 4 channel MKS 247 managing four MKS mass flow controllers (MFC), set in the range 0–200 sccm and (ii) Environics S4000 (Environics, Inc.) flow controller, comprising three MFCs supplying different flow rates (up to 500, 250 and 25 sccm, respectively), managed by its own software. Pure air (5.0) (Praxair–Rivoira, Italy) was used as gas carrier. A homemade PTFE (polytetrafluoroethylene) permeation tube filled with a suitable amount of Hg⁰ was included within such a delivery system to get set dilutions of Hg-saturated vapours. The tube was immersed in a thermostatically controlled bath, thus the desired Hg⁰ concentration delivered to the sensor was achieved by both tuning the temperature of the permeation tube and the dilution flow. The Hg⁰ concentration was checked by Tekran®2537A analyzer. Responses were calculated as $\Delta I/I_0$, where ΔI was the current variation and I_0 was the current when synthetic pure dry air was flowed. Sensor was restored after a quick thermal shot at 450°C under flow of pure air.

3 Results and Discussion

Nonwoven mats made of PVP and amorphous TiO_2 were obtained by the combination of electrospinning and sol-gel techniques (Fig. 1). The ES deposition was proceeding for 20 min on oxidized silicon wafers and IDEs, properly fixed on the surface of a conducting and rotating collector to form nanofibrous layers characterized by high surface areas and relatively small pore sizes (Zampetti et al., 2013). By changing the deposition time, both thickness and consistence of the mats changed. More specifically a 1h-deposition provided the formation of a thicker white and soft fabric, hygroscopic, soluble in both water and polar solvents and easily peeled off (Fig.1); instead a 20 min-deposition generated a fibrous film adhering to substrates, too thin to be weeded, thus preferred for sensors fabrication. The calcination process caused a complete degradation of PVP with formation of crystalline TiO_2 (*anatase*) and a significant shrinkage of fibers dimension (60-80 nm diameter, 5-40 nm grain size). Exploiting the photocatalytic properties of titania (*anatase*), a tunable decoration of fibers with gold nanoparticle could be achieved by dipping the fibrous mats in a proper aqueous solution (HAuCl_4 , PVP) under UV light irradiation (Li et al, 2004; Macagnano et al., 2015). The photocatalytic reaction was proved by the color change of the solution (red purple from light yellow) (Fig.1). Changing both UV irradiation exposure time and PVP concentration, as capping reagent, morphology, size and density of gold nanoparticles could be tuned (Macagnano et al., 2017).

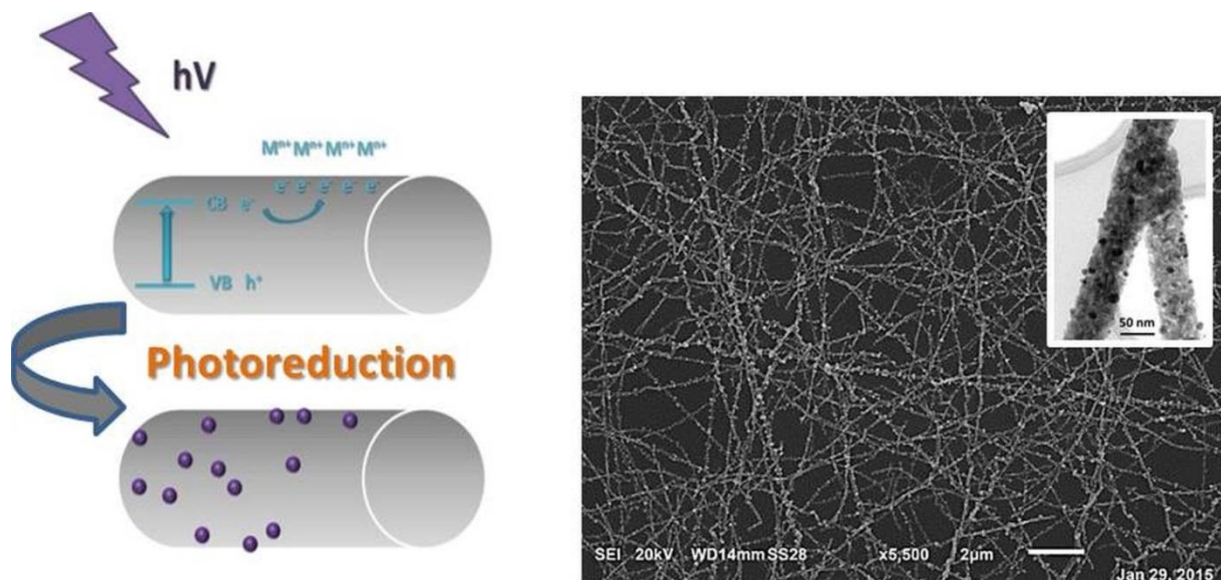
15



20 **Figure 1. Sketch of an electrospinning set-up comprising a syringe and a grounded rotating cylinder collector where the samples take place for their coverage (left); a piece of a nanofibrous fabric of TiO_2/PVP removed from the substrate after 1 h of electrospinning deposition (centre); a red-purple aqueous solution of $\text{HAuCl}_4/\text{PVP}$ after UV-light irradiation treatment holding a piece of the nanofibrous fabric of TiO_2 (*anatase*) obtained after TiO_2/PVP annealing (right)**

In the present work, among a series of differently coated fibrous layers, only the fibrous nanocomposites that were conductive at room temperature were selected and then their electrical and sensing features investigated. The controlled gold deposition was due to the photo-excited electrons on the surface of TiO_2 nanofibers that were able to reduce the gold ions thus inducing gold metal deposition (Fig. 2, *the sketch*). The capping reagent was responsible of the shape of the particles. The surfaces of nanofibers, as observed in SEM micrographs (Fig.2, *right*), appeared densely decorated with globular nanoparticles. In C-TEM image (Fig.2, *inset*) the gold nanoparticles appeared darker with spherical or quasi-spherical shapes. The single particles sizes were ranging between 2 and 20 nm, with a 7.8 ± 3 nm average diameter [(Macagnano et al.,

2017). Gold nanoparticles grew directly onto the nanofibers and their adhesion appeared relatively strong (despite due to van der Waals forces), since they both resisted to water rinsing and fibers scratching for TEM analyses.



5 **Figure 2.** A sketch of the photocatalytic process occurring on the fibers surface (*left*); SEM picture of a dense nanofibrous network of AuNPs/TiO₂ coating a silicon wafer (*right*); a C-TEM micrograph of fibers finely decorated with gold nanoparticles (*the darkest ones*) bound without using any additional linker (*inset*).

As a result of the photocatalytic process, the white porous mat became purple-violet. As reported in the spectrum of the AuNP/TiO₂ hybrid system, a characteristic absorbance band appeared at about 543 nm, which corresponded to the surface plasmon resonance (SPR) of the AuNPs (Sun et al, 2003). A red shifting and broadening of the absorbance band was observed with the increasing in AuNP size and fiber loading, respectively (data not shown). The colour is strictly depending on the size of the nanoparticles, and then their agglomeration at the solid state. According to Bui et al. (2007), such a band broadening phenomenon is due to the electric dipole–dipole interactions and coupling occurring between the plasmons of neighbouring particles, whereas nanoparticle agglomeration phenomena occurred.

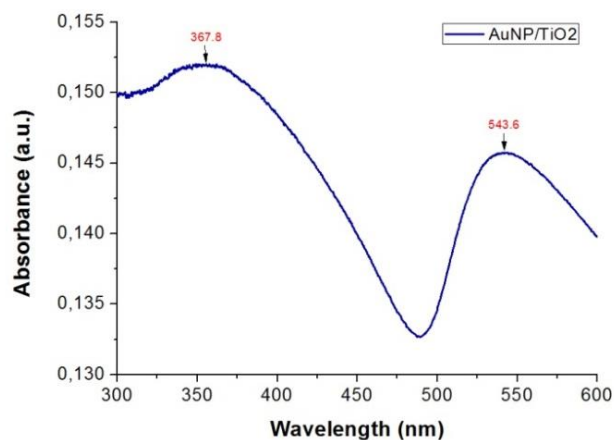


Figure 3. UV-Vis spectrum of a titania nanofibrous network after gold decoration (TiO₂: 367.8 nm; Au NPs: 543.6 nm)

Due to these features, UV-Vis absorption spectroscopy has been used in literature as a technique to reveal the changes in size, shape and aggregation of metal nanoparticles in liquid suspension after exposure to heavy metals, as Hg⁰ (Morris et al., 2002). Both blue-shifted wavelength and its extent were proportional to the amount of Hg⁰ that entered the liquid suspension. Similarly, when the gold decorated nanofibers of titania, collected on a quartz slice, were exposed to Hg⁰ vapours (2 ppm) in air for 15 min, a significant blue shifting was reported (~ 3 nm) (Fig. 4) due to the atomic adsorption of GEM on the surface. The nanoparticles could be regenerated by heating the sample at 550°C for 3 min, thus removing all the Hg⁰ adsorbed. Their recovery was stated by the achieving of the original values of wavelength (UV-Vis spectra). The regeneration process could be carried out for dozen times without any noticeable NPs deterioration. Similarly, the TiO₂ nanofibrous layers coating the metal electrodes of the transducers (Fig. 5), changed their colour after photocatalytic treatment (from white to pink).

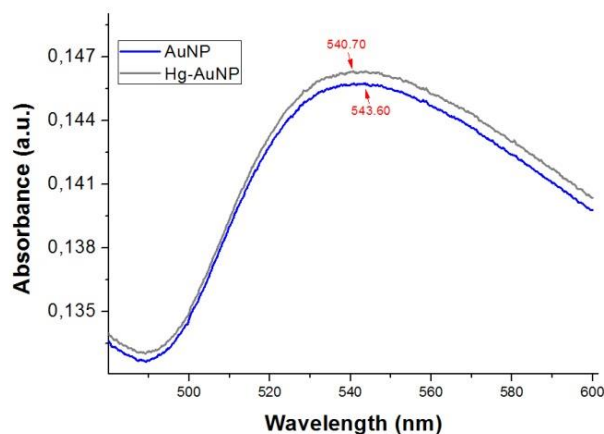


Figure 4. UV-Vis spectra of AuNPs/TiO₂ nanofibers before (*blue*) and after a 15 min exposure to 2 ppm of Hg⁰ (*gray*)

The IDE layout (Fig.5) comprises a set of interdigitated electrodes which occupies an area approximately 3x5 mm, completely coated with the sensitive fibers, and two bonding pads (2x2 mm) that will be connected to the electrometer (DC voltage). Such a planar interdigitated electrode configuration is the most commonly used for conductometric sensing applications.

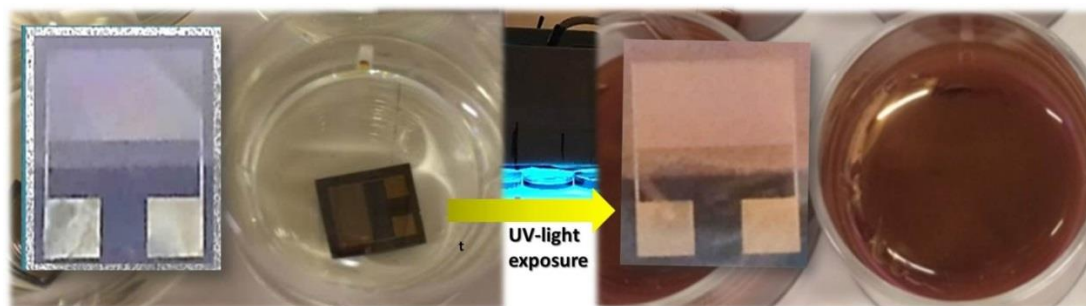


Figure 5. Chemosensor fabrication and final structure: IDE dipped (*left*) and exposed to UV-light (*right*) for gold decoration

Figure 6 depicts a Current–Voltage (I–V) curve of a chemosensor, under synthetic dry air flow. However curve shape was unaltered when air or nitrogen were flushed over the fibers (Macagnano et al., 2015), suggesting that oxygen concentrations poorly affected the electrical properties of such a chemoresistor. The resistance value of IDE coated with TiO₂ nanofibers before photocatalysis, resulted to be too high at room temperature to contribute straight to the final current value. The resulting linear shape (Ohmic behaviour) within the selected voltage range (from –3V to +3V) showed a constant resistance value for the sensor. The very low value of resistance (~1.2 kΩ) provided the chance to work at low voltage, with consequent effects on the energy consumption as well as lifetime of the material. Moreover, the linearity of I–V curve let us

suppose that the sensing scaffold had a good adhesion to the metal electrodes. The electron conductivity has been supposed occurring according to the percolation model (Macagnano et al., 2017; Muller et al., 2003), since the titania at room temperature was expected to be an insulating matrix. When it is metal doped, the electron conductivity is ruled by thermally activated electron tunnelling from one metal island (gold nanoparticles) to the other. However, the conductivity of the nanocomposite is lower than that of pure metal (gold) because the electron mean free path is greatly reduced due to the presence of the dielectric (the titania crystals). The electrical features, such as the reproducibility of the fabrication process, of this conductive device have been previously investigated by the authors (Macagnano et al., 2017; 2015a), showing encouraging results for the development of a low cost sensor for mercury detection. However, in spite of the high sensitivity (LOD: 2ppt) of the sensor, too long response time was necessary to detect traces of Hg^0 , overall if compared to the monitoring instrumentations (Ghaedi et al., 2006; Sanchez-Rodas et al., 2010; Ferrua et al., 2007) commonly involved in GEM detection. The long time in response was supposed to be in part due to the layout of the measuring system, since previously the sensor was housed in a quartz bottle of 100 ml volume. In fact an additional time is caused by the adsorption of Hg^0 traces from the surrounding environment (measuring chamber) up to achieve a sufficient number of Hg^0 atoms adsorbed on the surface sensor up to be electrically revealed. However, this sensor looks extremely encouraging if compared to other sensors currently involved in detecting mercury in air (Drelich et al., 2008; Kabir et al., 2015; Sabri et al., 2009; Mohibul Kabir et al., 2015; Raffa et al., 2006; James et al., 2012-2013; Chemnasiri et al., 2012; Sabri et al., 2011; Keebaugh et al., 2007; Crosby, 2013; McNicholas et al., 2011).

Many sensors have been designed and investigated to detect the several forms of mercury. Most of them have exploited the strong affinity between mercury and gold (Ford and Pritchard, 1971; Joyner and Roberts, 1973). Several studies have documented changes in the electrical properties, work function, and resistance of thin gold films upon exposure to various concentration of mercury vapor. For instance, an array of microcantilevers with different size, developed by Drelich et al., (2008), could measure different ranges of mercury concentration (between 37 and 700 $\mu\text{g}/\text{m}^3$), and were capable of revealing up to 10 pg Hg^0 adsorbed. However, their sensing system required both a dust-free gas carrier and a heating procedure (350 °C for 20 min) to regenerate the sensors. Gold-based conductometric sensors, too, have been designed and used to reveal mercury vapor through their electrical resistance changes (Raffa et al., 2006), but their sensitivity seemed often poor (about 1 $\mu\text{g}/\text{m}^3$). Quartz crystal microbalances (QCMs) devices, too, have been used as Hg^0 vapor sensors (Sabri et al., 2009) due to their high portability and selectivity, and no need for sample pre-treatments. Their absorptive capacity resulted improved (700 ng cm^{-2}) when the gold electrodes were made rough (more binding sites). However, additionally to the natural affinity of gold for mercury, the increased facility for producing and depositing nanoparticles with noble metals facilitated their use as possible sensors, overall in aqueous environments (Nolan and Lippard, 2008; Chemnasiri and Hernandez, 2012; Ratner and Mandler, 2015; Dong et al., 2015). James et al. (2012) developed a high sensitive chip working in a LSPR mode, based on gold nanoparticles (5 nm diameter) to monitor Hg^0 vapors. Such a system was able to linearly detect mercury concentrations from 1 to 825 $\mu\text{g}/\text{m}^3$, but it was strictly related to the flow rate: increasing the flow velocity (and mass transfer rate) increased the peak shift rate. The time resolution was limited by the rate of adsorption, which increased with

Reynolds number: at the greatest flow rate tested (57 LPM), an ambient mercury measurement (1 ng/m^3) needed 410 h to shift 1 nm, but accelerating the flow rate the time resolution could be reduced.

Gold thin film technology has been recently adopted in a commercial portable device to detect mercury (Jerome® J405 Mercury Vapor Analyzer), with a $0.01 \mu\text{g/m}^3$ resolution and a $750 \pm 50 \text{ cc/min}$ flow rate (www.azi.com). A series of scrubbers and filtering systems are able to reduce the effects of interferences to the gold-mercury interaction. The flow rate and the measuring system layout resulted as key parameters into the proper working of the device. These features seem to be significant also for the ES-based chemosensor.

The measuring chamber was designed in order to reduce the volume (0.7 ml) and to expose the fibers to the gas entry (Fig. 7). Such a measuring layout was designed to allow the fibrous network to be exposed to the mercury atoms as delivered into the sensor chamber.

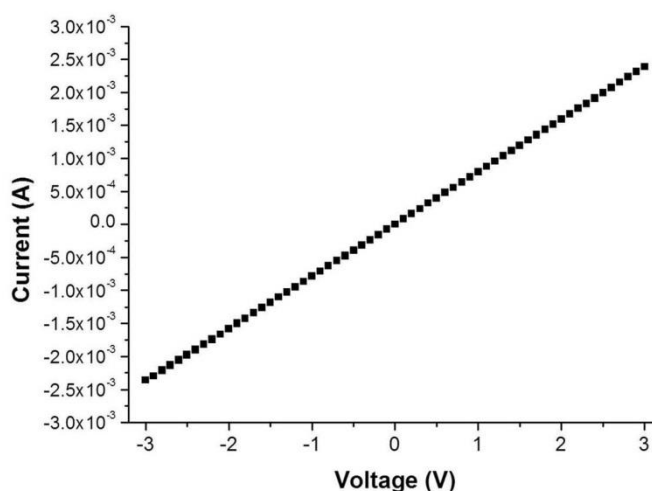


Figure 6. Chemosensor current-voltage curve

Sensing measurements, i.e. the current (or resistance) changes, were carried out in a continuous mode. The sensor measurements resulted in a change of the whole current (or resistance, i.e. $I = V/R$) according to Ohm's law. Firstly, the sensor was exposed to a flow of Hg^0 in air with a concentration of 800 ppb_v for 1 min (Fig. 7, right), and then air was flowed through the measuring chamber to clean the sensor surface. A rapid decrease in current was recorded ($1.056 \cdot 10^{-7} \text{ A} \cdot \text{s}^{-1}$) when Hg^0 entered the measuring chamber. The current curve trend slightly changed when clean air entered, quickly stabilizing to about the same current values reached for Hg^0 adsorption. Such an effect was probably due to the Hg^0 still housed inside the delivering tubes. The polluted line contribution was confirmed by further measurements (data not shown), where the slow current decrease completely disappeared when clean air never passed through part of tubes that had carried Hg vapors. Due to the strong affinity between Au and Hg^0 , a 3 min-thermal treatment was necessary to remove mercury from layer and get the same starting current value.

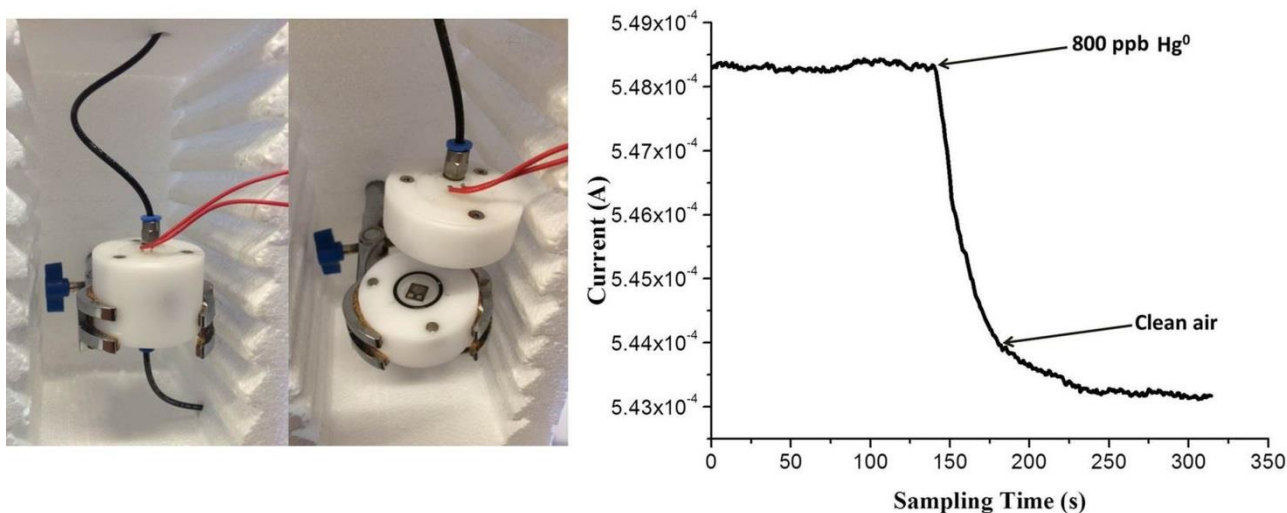
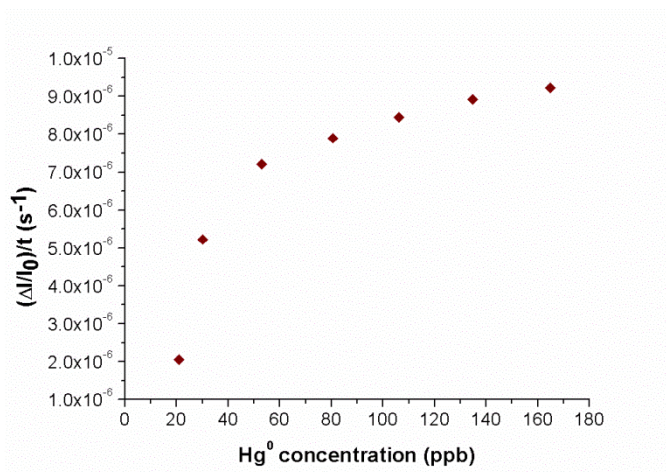


Figure 7. Homemade measurement chamber to house the chemosensor for laboratory experiments (left); plot depicting the transient response curve to 800 ppb Hg⁰ (V=0.3 V)



5 Figure 8. The normalized sensor response rate to the increasing concentration of vapour elemental mercury

Figure 8 depicts the normalized sensor response rate, i.e. the normalized current change per second, toward the increasing concentration of GEM (ranging between 20 and 160 ppb_v). Within this study, the selected flow rate was kept at 50 sccm in order to avoid turbulence effects. The resulting logarithmic curve describes the relationship between Hg⁰ concentration and the response time: small variations of Hg⁰ concentration up to 80 ppb_v were able to deeply change the response rate, on the
 10 contrary higher concentration seemed to affect only weakly this sensing feature. Thus, since a strong relationship is recorded between the concentration and the response time under 80 ppb_v of mercury, it is possible to find a correlation between the slope of the transient responses within the early minutes of the sensor response and well definite concentrations of Hg⁰ in air.

Figure 9 depicts the linear fitting of 10 min-sensor responses when increasing concentrations of mercury were flowed over the sensor. Related data were reported in Table 1.

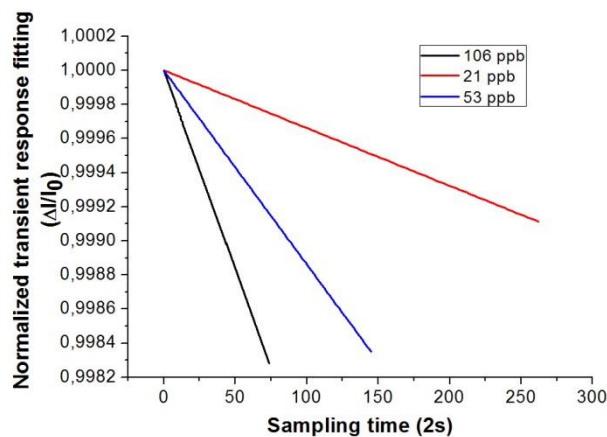


Figure 9. Linear fitting of the normalized sensor response within the first ten minutes

Table 1. Linear fitting parameters of 10 min-sensor responses to $21 \text{ ppb} \leq [\text{Hg}^0] \leq 106 \text{ ppb}$

ppb _v	$(\Delta I/I_0)s^{-1}$	SE (\pm)	R ²
21	-7.12602E-10	1.75521E-11	0.86
33	-1.50647E-9	1.05521E-10	0.91
39	-1.78067E-9	1.02615E-10	0.91
40	-1.85901E-9	1.01833E-10	0.92
53	-2.44657E-9	4.24993E-11	0.91
70	-3.19082E-9	2.55882E-11	0.93
106	-4.83599E-9	2.67462E-10	0.88

5

A linear relationship has been reported between the response rate and the concentration of Hg, according to the following equation (1):

$$y = (-4.56226E^{-11}) \cdot [\text{Hg}^0], [\text{Hg}^0] < 100 \text{ ppb}; SE: \pm 1.504E^{-12}; R^2 = 0.99675 \quad (1)$$

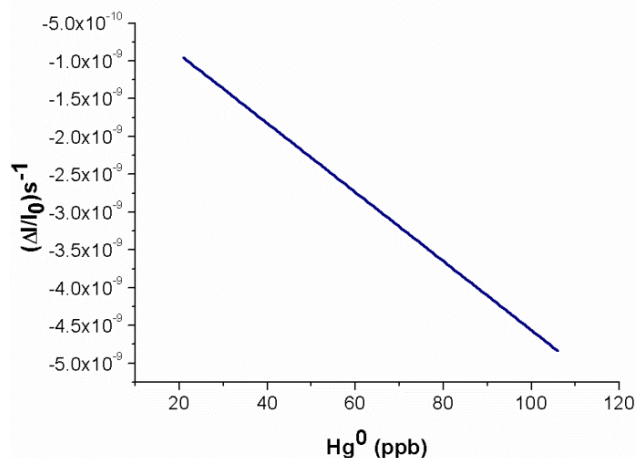


Figure 10. Linear relationships between the normalized response time and the Hg⁰ concentration, within the range of 20 and 100 ppb_v.

5 Therefore when the concentration of Hg increased, the response curve slope changed too linearly, allowing a limit of detection of about 1 ppb_v for a 10 min-exposure (50 sccm). About main interfering compounds, since at room temperature and in dark condition the measured current is supposed to be due to AuNPs decorating titania fibers, only chemical compounds interacting with gold are expected to be mostly responsible of the current changes (i.e. halides and sulphides). Thus in a blend of other chemicals, this sensor has been designed as a pretty selective sensor, being able to greatly decrease

10 the environmental disturbances allowing the investigator/manufacturer to design and then fabricate easier strategies to prevent contaminations from environment (selective filtering systems or coatings). Among common potential contaminants authors investigated previously water vapour influence (%RH) reporting no-effects on the electrical signals (Macagnano et al., 2015).

4 Conclusions

15 The adopted sensing strategy has focused on the strong affinity of mercury to gold combined to the nanostructures properties. Exploiting the photocatalytic properties of electrospun titania nanofibers, a novel conductometric sensor has been designed and fabricated to detect GEM in air. Electrospinning technology has been used successfully to create a 3D-framework of titania covering the electrode sensing area of the properly designed chemoresistors (IDEs). Exploiting the photocatalytic properties of titania AuNPs have been grown on nanofibers. Such a sensor was able to work at room

20 temperature and was sensitive to Hg⁰ also after a few minutes of exposure to polluted air. Since it is composed of titania and gold, it sounds to be robust and resistant to common solvents and VOCs commonly in the air (as reported by literature). Preliminary results suggest that the short thermal treatments, necessary to desorb mercury from AuNPs, didn't seem to affect the electrical properties of the device. Depending on the strategy of sampling, a sensing device based on such a chemosensor,

could be designed for real applications, specifically for real time monitoring of polluted sites. Few minutes of air sampling are sufficient to quantify the concentration of mercury in the air, in the range between 20-100 ppb_v (LOD: 1 ppb), without using traps or gas carriers. Changing parameters as the flow rate and the density and size of gold particles are expected to be significant parameters to improve the LOD and the response time, respectively. Finally, a modified transducer layout could be designed to exploit better the adsorptive capacity of the 3D-nanofibrous framework. However further investigations are necessary also to assess the effects of physical parameters of the environment, such as temperature fluctuations and UV-light (that should activate titania surface in adsorbing oxidized Hg), as well as chemical ones, such as volatile organic compounds and gas (like halides and sulphides) which are well known interfering of the adsorption process of the Hg⁰ on gold.

10 Acknowledgments

The activity is part of the International UNEP-Mercury Programme (UNEP-Mercury Air Transport and Fate Research (UNEP-MFTP) within the framework Global Mercury Observation System, funded by EC as part of EC FP7. Furthermore, authors gratefully thank Mr. Giulio Esposito and Mr. A. Capocecera for their support in the use of laboratory instrumentations and Mrs. A.R. Taddei of Univeristy of Tuscia (VT-Italy) for providing SEM and TEM micrographs.

15

References

- Bui, M.P., Baek, T.J., Seong, G.H., 2007. Gold nanoparticle aggregation-based highly sensitive DNA detection using atomic force microscopy. *Anal. Bioanal. Chem.* 388, 1185–1190
- Chemnasiri, W., Hernandez, FE., 2012. Gold nanorod-based mercury sensor using functionalized glass substrates, *Sensors and Actuators B* 173, 322–328
- Crosby, J., 2013. Mercury Detection with Gold Nanoparticles. Electronic Thesis and Dissertations UC Berkeley <http://eprints.cdlib.org/uc/item/3s40h5m0>
- Dong Z-M., Qing X-M., Zhao G-C., 2015. Highly Sensitive EQCM Sensor for Mercury Determination by Coupled Stripping Voltammetry. *Int J Electrochem Sci* 10 2602 – 2612
- 25 Drelich, J., White, C. L., Xu, Z., 2008. Laboratory Tests on Mercury Emission Monitoring with Resonating Gold-coated Silicon Cantilevers. *Environ. Sci. Technol.* 42 2072–2078
- Ferrua, N., Cerutti, S., Salonia, J. A., Olsina, R. A. and Martinez, L. D., 2007. On-line preconcentration and determination of mercury in biological and environmental samples by cold fiber-atomic absorption spectrometry. *J. Hazard. Mater.* 141 693–699
- 30 Ford, R.R., Pritchard, J., 1971. Work functions of gold and silver films. Surface potentials of mercury and xenon. *Trans. Faraday Soc.* 67 216–221
- Ghaedi, M., Fathi, MR., Shokrollahi, A., Shajarat, F., 2006. Highly Selective and Sensitive Preconcentration of Mercury Ion and Determination by Cold Fiber Atomic Absorption Spectroscopy. *Analytical Letters* 39, 1171-1185
- Gustin, M.S., Huang, J., Miller, M.B., Peterson, C., Jaffe, D.A., Ambrose, J., Finley, B.D., Lyman, S.N., Call, K., Talbot, R., Feddersen, D., Mao, H., Lindberg, S.E., 2013. Do we understand what the mercury speciation instruments are actually measuring? Results of RAMIX. *Environ. Sci. Technol.* 47, 7295-7306.
- 35 Gustin, M.S., Lyman, S.N., Kilner, P., Prestbo, E., 2011. Development of a passive sampler for gaseous mercury. *Atmos. Environ.* 45, 5805-5812.

40

- Harner, T., Farrar, N.J., Shoeib, M., Jones, K.C., Gobas, F., 2003. Characterization of polymer-coated glass as a passive air sampler for persistent organic pollutants. *Environ. Sci. Technol.* 37, 2486-2493.
- Hedgecock, I., Pirrone, N., Sprovieri, F., Pesenti, E. (2003) Reactive Gaseous Mercury in the Marine Boundary Layer: Modeling and Experimental Evidence of its Formation in the Mediterranean. *Atmospheric Environment*, 37/S1, 41-49.
- 5 Huang, J., Lyman, S.N., Hartman, J.S., Gustin, M.S., 2014. A review of passive sampling systems for ambient air mercury measurements. *Environ. Sci. Process. Impacts* 16, 374-392.
- James, J.Z., Lucas, D., Koshland, C.P., 2012. Gold Nanoparticle Films As Sensitive and Reusable Elemental Mercury Sensors. *Environ. Sci. Technol.* 46 (2012) 9557–9562
- 10 James, JZ., Lucas, D., Koshland, C.P., 2013. Elemental mercury fiber interaction with individual gold nanorods, *Analyst* 138, 2323-2328
- Joyner R.W., Roberts M.W., 1973. Auger electron spectroscopy studies of clean polycrystalline gold and of the adsorption of mercury on gold. *J. Chem. Soc. Faraday Trans. 1 Phys. Chem. Condens. Phases* 69 1242–1250
- 15 Kabir, K., Sabri, Y., Matthews, G., Jones, L., Ippolito, S., Bhargava, S. 2015. Selective detection of elemental mercury fiber using a surface acoustic wave (SAW) sensor. *Analyst*, 140, 5508-5517
- Keebaugh, S., Nam, W.J., Fonash, S.J., 2007. Manufacturable Highly Responsive Gold Nanowire Mercury Sensors, *NSTI-Nanotech* 3, 33-36, www.nsti.org
- Li, D., McCann, J.T., Gratt, M., Xia, Y., 2004. Photocatalytic deposition of gold nanoparticles on electrospun nanofibers of titania, *Chemical Physics Letters* 394, 387–391
- 20 Lyman, S.N., Gustin, M.S., Prestobo, E.M., 2010. A passive sampler for ambient gaseous oxidized mercury concentrations. *Atmos. Environ.* 44, 246-252.
- Macagnano, A., Zampetti, E., Kny, E., 2015b. *Electrospinning for High Performance Sensors*, Springer International Publishing, pp. 1-329.
- Macagnano, A., Zampetti, E., Perri, V., Bearzotti, A., Sprovieri, F., Pirrone, N., Esposito, G., De Cesare, F., 2015a. Photocatalytically Decorated Au-nanoclusters TiO₂ Nanofibers for Elemental Mercury Fiber Detection, *Procedia Engineering* 120, 422–426
- Macagnano, A., Perri, V., Zampetti, E., Bearzotti, A., Ferretti, A.M., Sprovieri, F., Esposito, G., Pirrone, N., De Cesare, F., 30 2017. Elemental mercury vapour chemoresistors employing TiO₂ nanofibers photocatalytically decorated with Au-Nanoparticles, *Sensor. Actuat. B-CHEM.* (*available on line*). <http://dx.doi.org/10.1016/j.snb.2017.03.037>
- McNicholas, T.P., Zhao, K., Yang, C., Hernandez, S.C., Mulchandani, A., Myung, N.V., Deshusses, M.A., 2011. Sensitive Detection of Elemental Mercury Fiber by Gold-Nanoparticle-Decorated Carbon Nanotube Sensors, *J. Phys. Chem. C* 115, 13927–13931
- 35 Mohibul Kabir, K.M., Ippolito, S.J., Matthews, G.I., Abd Hamid, S.B., Sabri, Y.M., Bhargava, S.K., 2015. Determining the Optimum Exposure and Recovery Periods for Efficient Operation of a QCM Based Elemental Mercury Fiber, *Sensor Journal of Sensors* 727432-9
- Morris, T., Klopper, K., Wilson, S., Szulczewsk, G., 2002. A Spectroscopic Study of Mercury Fiber Adsorption on Gold Nanoparticle Films, *Journal of Colloid and Interface Science* 254, 49–55
- 40 E. M. Nolan E.M., S. J. Lippard S.J., 2008. Tools and tactics for the optical detection of mercuric ion. *Chem. Rev.* 108 (9) 3443–3480

- Pacyna, E., Pacyna, J., Sundseth, K., Munthe, J., Kindbom, K., Wilson, S., Steenhuisen, F., and Maxson, P.: Global emission of mercury to the atmosphere from anthropogenic sources in 2005 and projections to 2020, *Atmos. Environ.*, 44, 2487–2499, doi:10.1016/j.atmosenv.2009.06.009, 2010.
- 5 Pirrone, N., Cinnirella, S., Feng, X., Finkelman, R., Friedli, H., Leaner, J., Mason, R., Mukherjee, A., Stracher, G., Streets, D., and Telmer, K.: Global mercury emissions to the atmosphere from anthropogenic and natural sources, *Atmos. Chem. Phys.*, 10, 5951–5964, doi:10.5194/acp-10-5951-2010, 2010
- Pirrone, N., Aas, W., Cinnirella, S., Ebinghaus, R., Hedgecock, I.M., Pacyna, J., Sprovieri, F., Sunderland, E.M., 2013.
10 Toward the next generation of air quality monitoring: mercury. *Atmos. Environ.* 80, 599-611.
- Plaisance, H., Piechocki-Minguy, A., Gracia-Fouque, S., Galloo, J.C., 2004. Influence of meteorological factors on the NO₂ measurements by passive diffusion tube. *Atmos. Environ.* 38, 573-580.
- 15 Pozo, K., Harner, T., Shoeib, M., Urrutia, R., Barra, R., Parra, O., Focardi, S., 2004. Passive-sampler derived air concentrations of persistent organic pollutants on a north-south transect in Chile. *Environ. Sci. Technol.* 38, 6529-6537.
- Raffa, V., Mazzolai, B., Mattoli, V., Mondini, A., Dario, P., 2006. Model validation of a mercury sensor, based on the resistivity variation of a thin gold film, *Sensors And Actuators. B* 114, 513-521
- 20 Ratner N., Mandler D., 2015. Electrochemical Detection of Low Concentrations of Mercury in Water Using Gold Nanoparticles. *Anal Chem* 87 5148–5155
- Sabri, Y.M., Ippolito, S.J., O'Mullane, A.P., Tardio, J., Bansal, V., Bhargava S.K., 2011. Creating gold nanoprisms directly on quartz crystal microbalance electrodes for mercury fiber sensing. *Nanotechnology* 22 (30) 305501
- Sabri, Y.M., Ippolito, S.J., Tardio, J., Atanacio, A.J., Sood, D.K., Bhargava, S.K., 2009. Mercury diffusion in gold and silver thin film electrodes on quartz crystal microbalance sensors. *Sensor. Actuat. B-CHEM* 137 246–252
- 25 Sánchez-Rodas, D., Corns, W.T., Chen, B., Stockwell, P.B., 2010. Atomic Fluorescence Spectrometry: a suitable detection technique in speciation studies for arsenic, selenium, antimony and mercury. *J. Anal. At. Spectrom.* 25 933-946
- Sderstrm, H.S., Bergqvist, P.A., 2004. Passive air sampling using semipermeable membrane devices at different wind-speeds in situ calibrated by performance reference compounds. *Environ. Sci. Technol.* 38, 4828-4834.
- 30 Sprovieri, F., Pirrone, N., Bencardino, M., D'Amore, F., Carbone, F., Cinnirella, S., Mannarino, V., Landis, M., Ebinghaus, R., Weigelt, A., Brunke, E.-G., Labuschagne, C., Martin, L., Munthe, J., Wängberg, I., Artaxo, P., Morais, F., H. J. Barbosa, J. Brito Cairns, W., Barbante, C., del Carmen Diéguez, M., Garcia, P. E., Dommergue, A., Angot, H., Magand, O., Skov, H., Horvat, M., Kotnik, J., Read, K. A., Neves, L. M., Gawlik, B. M., Sena, F., Mashyanov, N., Vladimir, Obolkin, A., Wip, D.,
- 35 Feng, X. B., Zhang, H., Fu, X., Ramachandran, R., Cossa, D., Knoery, J., Maruszczak, N., Nerentorp, M., and Norstrom, C., 2016a. Atmospheric Mercury Concentrations observed at ground-based monitoring sites globally distributed in the framework of the GMOS network, *Atmos. Chem. Phys.*, 16, 1–21.
- Sprovieri, F., Pirrone, N., Bencardino, M., D'Amore, F., Angot, H., Barbante, C., Brunke, E.G., Arcega-Cabrera, F., Cairns, W., Comero, S., Diéguez, M., Dommergue, A., Ebinghaus, R., Feng, X.B., Fu, X., Garcia, P. E., Gawlik, B. M., Hageström, U., Hansson, K., Horvat, M., Kotnik, J., Labuschagne, C., Magand, O., Martin, L., Mashyanov, N., Mkololo, T., Munthe, J., Obolkin, V., Islas M.R, Sena, F., Somerset, V., Spandow, P., Vardè, M., Walters, C., Wängberg, I., Weigelt, A., Yang, X., Zhang, H. 2016b. Five-year records of Total Mercury Deposition flux at GMOS sites in the Northern and Southern Hemispheres *Atmos. Chem. Phys. Discuss.*, doi:10.5194/acp-2016-517
- 45 Sun, Y., Xia, Y., 2003. Gold and silver nanoparticles: A class of chromophores with colors tunable in the range from 400 to 750 nm. *Analyst* 128, 686–691.
- Y Yuan, Y., Zhao, Y., Li, H. Li, Y., Gao, X., Zheng, C., Zhang J., 2012. Electrospun metal oxide–TiO₂ nanofibers for elemental mercury removal from flue gas, *Journal of Hazardous Materials*, 227–228, 427–435

Zampetti, E., Pantalei, S., Muzyczuk, A., Bearzotti, A., De Cesare, F., Spinella, C., Macagnano, A., 2013. A high sensitive NO₂ gas sensor based on PEDOT-PSS/TiO₂ nanofibers, *Sensors and Actuators B* 176, 390-398

Zhang, W., Tong, Y.D., Hu, D., Ou, L.B., Wang, X.J., 2012. Characterization of atmospheric mercury concentrations along an urban-rural gradient using a newly developed passive sampler. *Atmos. Environ.* 47, 26-32.

5